# Structure of Bacterial Regulatory RNAs Determines Their Performance in Competition for the Chaperone Protein Hfq

Ewelina M. Małecka, Joanna Stróżecka, Daria Sobańska, and Mikołaj Olejniczak*

Institute of Molecular Biology and Biotechnology, Faculty of Biology, Adam Mickiewicz University in Poznań, Umultowska 89, 61-614 Poznań, Poland

Ⓢ Supporting Information

**ABSTRACT:** Bacterial regulatory RNAs require the chaperone protein Hfq to enable their pairing to mRNAs. Recent data showed that there is a hierarchy among sRNAs in the competition for access to Hfq, which could be important for the tuning of sRNA-dependent translation regulation. Here, seven structurally different sRNAs were compared using filter-based competition assays. Moreover, chimeric sRNA constructs were designed to identify structure elements important for competition performance. The data showed that besides the 3′-terminal oligouridine sequences also the 5′-terminal structure elements of sRNAs were essential for their competition performance. When the binding of sRNAs to Hfq mutants was compared, the data showed the important role of the proximal and rim sites of Hfq for the binding of six out of seven sRNAs. However, ChiX sRNA, which was the most efficient competitor, bound Hfq in a unique way using the opposite—distal and proximal—faces of this ring-shaped protein. The data indicated that the simultaneous binding to the opposite faces of Hfq was enabled by separate adenosine-rich and uridine-rich sequences in the long, single-stranded region of ChiX. Overall, the results suggest that the individual structural composition of sRNAs serves to tune their performance to different levels resulting in a hierarchy of sRNAs in the competition for access to the Hfq protein.

B acterial *trans*-encoded small regulatory RNAs (sRNAs) participate in the cell's response to changes in environmental conditions[1,2] and are involved in the regulation of the virulence of pathogenic species.[3,4] The role of the majority of sRNAs is to repress or activate translation of selected mRNAs. They exert this effect by binding to partly complementary sequences in the target mRNAs, which changes the availability of these mRNAs for the ribosome.[5,6] The binding of most sRNAs to their targets is critically dependent on a chaperone protein Hfq, which facilitates the base-pairing between the complementary sequences of sRNAs and mRNAs.[1]

The *Escherichia coli* chaperone protein Hfq interacts with sRNAs and mRNAs using several binding sites, which were identified on its proximal and distal surfaces, as well as on the rim of this ring-shaped protein.[7−11] The site on the proximal face binds uridine-rich RNA sequences, such as the 3′-terminal uridine tails of sRNAs remaining from Rho-independent termination sites.[7,8,12,13] The distal face contains a circular binding site for adenosine-rich RNAs,[8,9,14] in particular those that contain $(AAN)_n$ sequence repeats, which are present in mRNAs binding to Hfq.[15−20] It was proposed that the proximal site serves to bring sRNA close to the regulated mRNA bound to the distal face, while the third RNA binding site, which has been recently identified on the rim of this protein,[10] plays an essential role in the annealing of sRNAs to mRNAs.[21] Interestingly, individual sRNA/mRNA pairs are differently dependent on the proximal, distal, and rim sites of Hfq for mRNA translation regulation *in vivo*,[22] which may reflect

different modes used by those sRNAs or mRNAs to bind to Hfq.
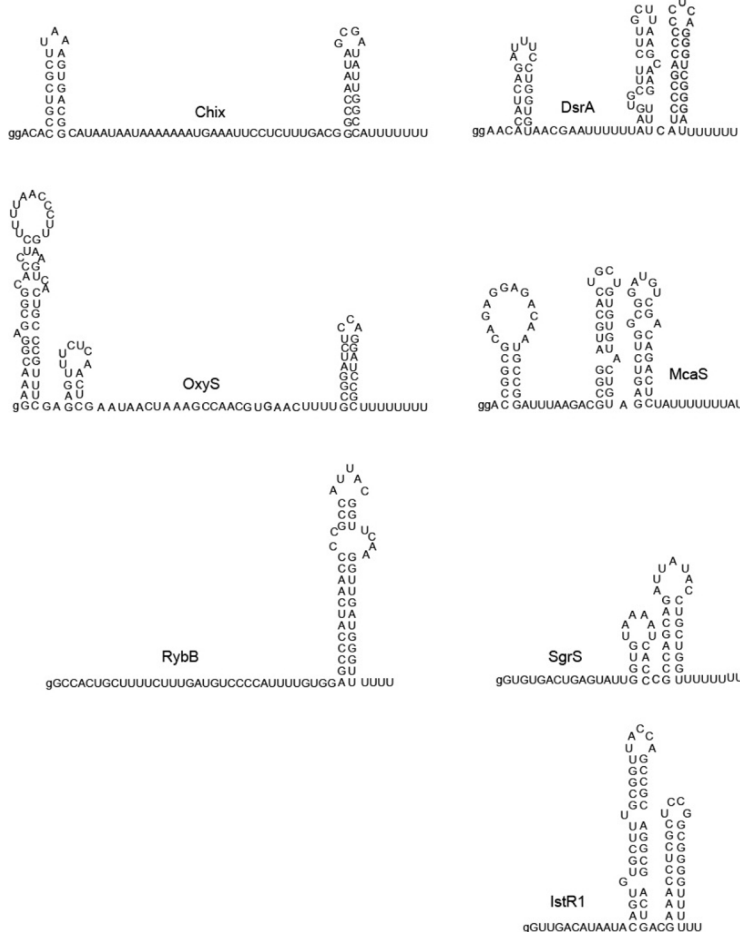
Regulatory RNAs compete for access to the Hfq protein in *E. coli* cells.[23,24] When Hfq was titrated in the cell to higher than natural concentrations, it resulted in the increase of the sRNA-dependent repression of translation.[23] This suggests that the Hfq concentration is limiting for translation regulation *in vivo*, which results in the competition among sRNAs for access to this protein. Moreover, when several sRNAs were overexpressed in cells they differed in the competition against other sRNAs in Hfq-dependent *rpoS* mRNA translation regulation.[24] These *in vivo* data could be explained by differences among sRNAs in their ability to gain access to Hfq in the presence of other sRNAs. Indeed, the results of *in vitro* competition assays showed that sRNAs differ in the ability to outcompete other sRNAs from the complex with Hfq.[25,26] It was recently proposed that sRNAs use an active mechanism to displace other sRNAs from the complex with Hfq.[25,27] Hence, despite the very tight binding and slow unassisted dissociation rates, the cycling of sRNAs on this protein occurs very rapidly in the presence of competing sRNAs or when the total sRNA concentration is increased.[25−27] Overall, these data suggest that sRNAs widely differ in their ability to gain access to Hfq, which
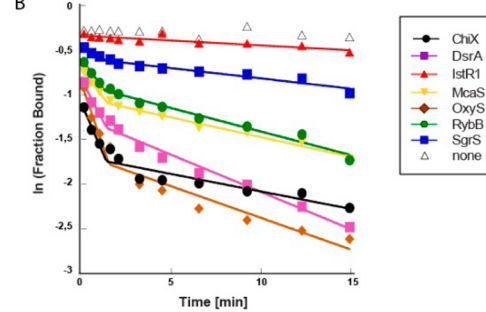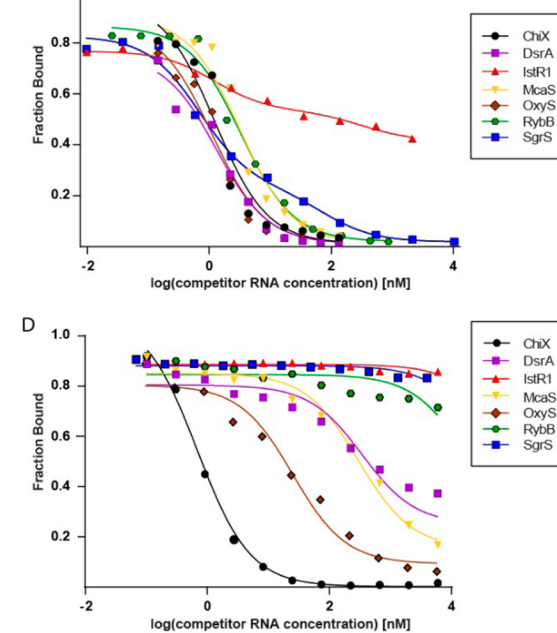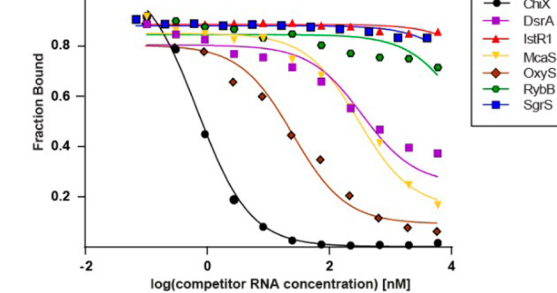
**Figure 1.** Structurally diverse sRNAs have different efficiencies in competition for Hfq. (A) Experimentally verified secondary structures of sRNAs DsrA,[29,41] RybB,[43] OxyS,[42] IstR1,[38] ChiX,[40] SgrS, and McaS (Supplemental Figure 1, Supporting Information); (B) the kinetics of dissociation of $^{32}$P-labeled DsrA RNA from Hfq induced by 3.75 nM concentration of unlabeled sRNA competitors. Fitting of the data presented in the graphs using segmental linear regression provided $k_{off}^1$ and $k_{off}^2$ values of, respectively, $78 \times 10^{-4}$ s$^{-1}$ and $6.5 \times 10^{-4}$ s$^{-1}$ for ChiX, $64 \times 10^{-4}$ s$^{-1}$ and $14 \times 10^{-4}$ s$^{-1}$ for DsrA, $43 \times 10^{-4}$ s$^{-1}$ and $7.4 \times 10^{-4}$ s$^{-1}$ for McaS, $98 \times 10^{-4}$ s$^{-1}$ and $12 \times 10^{-4}$ s$^{-1}$ for OxyS, and $45 \times 10^{-4}$ s$^{-1}$ and $8.8 \times 10^{-4}$ s$^{-1}$ for RybB. Linear fitting of the data for IstR1 and SgrS provided $k_{off}$ values of $1.8 \times 10^{-4}$ s$^{-1}$ and $4.5 \times 10^{-4}$ s$^{-1}$, respectively; (C) equilibrium assay monitoring competition of unlabeled sRNAs against $^{32}$P-DsrA bound to Hfq. The best fits of data show the IC$_{50}$ values of 1 nM for ChiX, 1.1 nM for DsrA, 2.8 nM for McaS, 0.93 nM for OxyS, 2.8 nM for RybB, 1 nM (IC$_{50}^{High}$) and 290 nM (IC$_{50}^{Low}$) for IstR1, 0.57 nM (IC$_{50}^{High}$) and 67 nM (IC$_{50}^{Low}$) for SgrS. (D) Equilibrium assay monitoring competition of unlabeled RNAs against $^{32}$P-ChiX bound to Hfq. The best fits of data show the IC$_{50}$ values of 0.67 nM for ChiX, 340 nM for DsrA, 300 nM for McaS, 25 nM for OxyS. The IC$_{50}$ values for IstR1, RybB and SgrS are estimated to be higher than 10 $\mu$M. Average $k_{off}$ and IC$_{50}$ values from at least three independent experiments are presented in Table 1. The fitting errors of individual data sets were significantly lower than the errors for the triplicates.

could affect the network of sRNA-dependent regulation of translation.

The structural differences among sRNAs could be one reason for the differences in the competition for Hfq. The *trans*-encoded Hfq-dependent sRNAs are typically composed of one or several stem-loops interspersed with single-stranded regions, which often contain AU-rich sequences thought to be involved in Hfq binding.[5] At the 3′ end they contain Rho-independent terminator stem-loops followed by uridine-rich sequences, which were found to be important for SgrS sRNA binding to Hfq.[13,28] Additionally, the presence of a stem-loop on either side of a single-stranded AU-rich sequence was found to be necessary for Hfq binding to DsrA sRNA.[29] In agreement with that, the U-rich sequences located in an internal single-stranded region, in a hairpin loop, and in a 3′-terminal region of Spot42

sRNA were protected against hydroxyl radical induced degradation in the presence of Hfq.[30] However, despite the overall similarity of sRNA structures, they differ in the length and sequence of single-stranded regions, the number of stem-loops and their position in relation to single-stranded regions, as well as their molecular size and sequence. Hence, it appears that intricate details of sRNA structures, possibly leading to different interactions with Hfq,[22,31] could explain the observed differences in their competition performance.

To elucidate the role of sRNA structure in competition for Hfq, the properties of natural *E. coli* sRNAs and the chimeric constructs composed of structural motifs derived from strong and weak competitors were analyzed in competition assays. Moreover, sRNA binding to wild type and mutated Hfq

proteins was analyzed to assess how the sRNA structure modulates their interactions with this protein.

## ■ MATERIALS AND METHODS

**Preparation of RNAs.** sRNA molecules used in this study were *in vitro* transcribed using T7 RNA polymerase and purified on a denaturing polyacrylamide gel as described.[26,32] The DNA templates for transcription were obtained by Taq extension of overlapping, chemically synthesized oligodeoxyribonucleotides (oligo.pl, Warsaw, Poland). RNAs were 5′-labeled using T4 polynucleotide kinase (Fermentas) and purified using P-30 spin columns. All wild type sRNAs contained a whole encoded 3′-terminal oligouridine sequence of the Rho-independent transcription terminator,[13] as shown in Figure 1. Chemically synthesized oligoribonucleotides $A_{27}$ and $U_{18}$ were kind gifts of Prof. Ryszard Kierzek (Institute of Bioorganic Chemistry, Polish Academy of Sciences, Poznań).

**Hfq Protein Expression and Purification.** The *E. coli* Hfq protein with His$_6$-tag at C-terminus was expressed from pET15b vector (Novagen) and purified as described[8] with the following modifications. After the overexpression of the Hfq protein, the cells were lysed by sonication, and the resulting lysate was clarified by centrifugation and loaded onto a HisTrap crude column charged with NiSO$_4$ (GE Healthcare). Proteins bound to the resin were eluted with a linear gradient of 35−600 mM imidazole in buffer A (50 mM HEPES, pH 7.5, 500 mM NH$_4$Cl, 5% (w/v) glycerol). To remove any residual nucleic acids, the fractions containing Hfq were pooled and treated with RNase A (30 μg/mL) and DNase I (5 U/mL) for 1 h at 37 °C. The solution was diluted to decrease the imidazole concentration and again passed over a Ni$^{2+}$ affinity column. Fractions after elution were concentrated and applied to a HiLoad 16/60 Superdex 200 size exclusion column (GE Healthcare) equilibrated with storage buffer (50 mM HEPES 7.5, 250 mM NH$_4$Cl, 1 mM EDTA, and 10% glycerol). The protein was eluted, concentrated if needed, and stored at −80 °C. The protein purity was assessed by SDS-PAGE and by measurement of the ratio of absorbance at 280 to 260 nm. The molecular weight of wild type Hfq protein was determined by MALDI-TOF as 11865.038 Da, which agrees with the calculated mass of 11989 Da after subtracting the molecular weight of the N-terminal methionine, which is often removed in the cells.[33] The protein concentration was determined using absorbance at 280 nm[8] and corrected for the active fraction using titration against $^{32}$P-RybB, $^{32}$P-ChiX, and $^{32}$P-$A_{27}$. The *hfq* mutations, introduced into pET15b-hfq carrying *hfq*, were generated by site-directed mutagenesis using specific primers as described,[22] and PfuTurbo Cx Hotstart DNA Polymerase (Agilent Technologies). Mutations were verified by sequencing. Mutated proteins were purified in the same way as wt Hfq.

**Equilibrium Binding Assay.** The double filter retention assay was used with top nitrocellulose and bottom charged nylon membranes and a modified dot blot filter apparatus.[34−36] The binding reactions were performed as described[26] in HB buffer (50 mM HEPES pH 7.5, 50 mM NaCl, 50 mM KCl, 2.5 mM MgCl$_2$, and 0.1 mM EDTA). To initiate the reaction, 25 μL of 5′-$^{32}$P-labeled RNA (0.1 nM concentration) was mixed with 25 μL of Hfq protein at a required range of concentrations. The reactions were incubated for 25 min at room temperature, and immediately afterward 45 μL of each reaction was filtered and washed with 100 μL of HB buffer. Filters were hot air-dried, exposed, and quantified using a phosphorimager and MultiGauge software (Fuji). The data

were fit to the binding isotherm assuming 1:1 stoichiometry (hyperbolic equation).[37] Standard deviations were calculated from at least three independent experiments.

**Dissociation Assay.** Dissociation kinetics was monitored using double filter retention assay as previously described,[26] except that dissociation was initiated only by adding unlabeled competitor RNA, without dilution of the binding mixture. *E. coli* Hfq protein (0.28 nM) was incubated with refolded 5′-$^{32}$P-labeled RNA (0.05 nM) for 20 min in HB buffer at RT. Dissociation reactions were simultaneously initiated by mixing 5 μL of 150 nM unlabeled competitor RNA with 195 μL of the binding reaction containing Hfq and 5′-$^{32}$P-RNA, using a multichannel pipet. Final concentration of unlabeled competitor RNA in the dissociation reaction was 3.75 nM. At indicated times 17 μL aliquots were withdrawn, filtered, and immediately washed with 100 μL of HB buffer. Membranes were dried and quantified using a phosphorimager and MultiGauge software (Fuji). Dissociation rates were calculated as described.[26]

**Equilibrium Competition Assay.** A required range of unlabeled competitor RNA concentrations was prepared in HB buffer by sequential dilution, and 10 μL of each concentration was transferred to new microplate wells. Subsequently, 10 μL of $^{32}$P-labeled RNA in 0.06 nM final concentration was added to competitor RNA. At the end 10 μL of Hfq protein in HB buffer was added to the above-mentioned mixture. Final concentrations in the IC$_{50}$ reaction were 2.2 nM Hfq, 0.04 nM $^{32}$P-labeled RNA, and unlabeled RNA at the indicated concentration range. After 35 min of incubation, 25 μL aliquots were filtered and washed with 100 μL of HB buffer. Membranes were dried, and the fraction of RNA bound was determined using a phosphorimager. The unlabeled competitor concentrations at which 50% of Hfq-bound $^{32}$P-labeled RNA was dissociated (IC$_{50}$ values) were calculated using GraphPad Prism software. It should be noted that the equations used are a way to approximate the competitor concentration, at which 50% of the radioactive label is displaced, but do not reflect the competition mechanism. The basic equation used for fitting the data was a competitive binding equation, assuming one site binding. The equation was $F_B = B + (A - B)/(1 + 10^{X - \log IC_{50}})$, where $F_B$ is a fraction bound, and $A$ and $B$ plateaus (top and bottom respectively) are in the units of the $Y$ axis. However, for the competition against $^{32}$P-$U_{18}$ and $^{32}$P-$A_{27}$ binding to Hfq (Figure 4) the data were fit using the equation $F_B = B + (A - B)/(1 + 10^{(\log IC_{50} - X) \times n})$, where $n$ is a Hill coefficient. Moreover, the presence of two RNA binding sites on Hfq was assumed when fitting the biphasic competition data (Figures 1, 2, and 3). The equation used was $F_B = B + ((A - B) \times F_H)/(1 + 10^{X - \log IC_{50}High}) + ((A - B) \times (1 - F_H))/(1 + 10^{X - \log IC_{50}Low})$, where $F_H$ is the fraction of $^{32}$P-RNA displaced from the sites bound by the unlabeled competitor RNA with higher affinity.

## ■ RESULTS

To test the effect of sRNA structure on their performance in competition for Hfq, seven *E. coli* sRNA molecules were selected, which were predicted to exhibit different competition efficiencies (Figure 1A). Recent *in vivo* data showed that ChiX and OxyS sRNAs were the most efficient, while RybB and SgrS were among the least efficient Hfq competitors in assays measuring competition against positive regulation of *rpoS* expression.[22] IstR1 was expected to be an example of a weak competitor based on previous *in vitro* studies,[23,24] and because its function is not dependent on Hfq *in vivo*.[38] McaS sRNA,

together with ChiX and DsrA, were the subjects of studies on the effect of mutations in Hfq on translation regulation *in vivo*, which could provide additional insights into their Hfq-dependent properties.[22] Importantly, these sRNAs have a modular architecture composed of well-defined structural elements,[39] which allows the design of chimeric molecules composed of elements transplanted from different sRNAs. The whole gene-encoded 3′-terminal oligoU sequences remaining from Rho-independent terminators were included in the sRNA structures (Figure 1A), because they were recently shown to be important for Hfq binding and translation regulation by sRNAs.[13,28] In the case of SgrS, a 5′-terminally truncated sequence was used, the same that was recently studied *in vivo*.[13,28] The secondary structures of ChiX,[40] DsrA,[29,41] IstR1,[38] OxyS,[42] and RybB[43] were previously determined (Figure 1A). The probing of the structure of SgrS using T2 and S1 RNases showed that it is composed of two stem-loops, and a 5′-terminal single-stranded region, as predicted before[13] (Figure 1A, Supplemental Figure 1A,B, Supporting Information). When the structure of McaS was probed the data were consistent with the most stable structure predicted by RNAstructure software,[44] according to which McaS is composed of three stem-loops (Figure 1A, Supplemental Figure 1C,D, Supporting Information). In comparison to the previously proposed *mfold*-predicted structure,[45] the middle stem-loop is located closer to the 3′-terminus, and the 3′-terminal stem-loop is shorter. Overall, these seven sRNAs provided remarkable structural and functional diversity, which made them good subjects to study the dependence between the structure of sRNAs and their performance in competition for Hfq.

**Structurally Diverse sRNAs Show Different Efficiencies in the Kinetic and Equilibrium Competition Assays.** The kinetics of displacement of 5′-$^{32}$P-labeled DsrA sRNA from its complex with Hfq by different unlabeled sRNAs were compared using a high-throughput filter retention assay (Figure 1B, Table 1). DsrA is a model sRNA, which has been used in numerous studies on the function of Hfq.[8,22,29,46,47] The assay was essentially performed as previously described,[26] except that the dissociation reaction was initiated only by the addition of
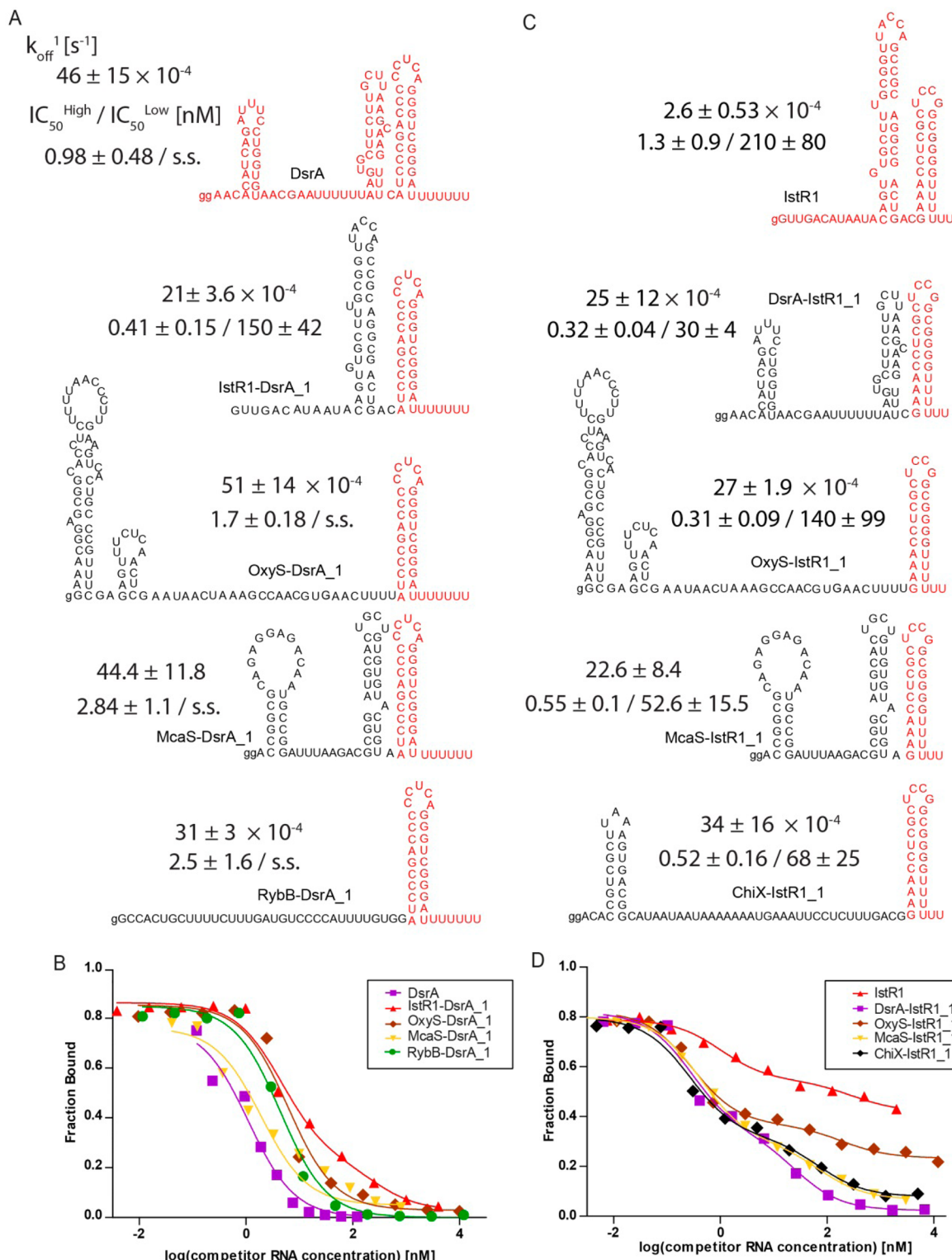
unlabeled competitor sRNA, without the simultaneous dilution of the reaction. This allowed a stronger radioactivity signal to be obtained in the assay and was not expected to affect the measured dissociation rates because the unassisted, dilution-only initiated dissociation was shown to occur very slowly.[25,26] The dissociation rate values ($k_{off}$) were obtained as negative slopes of linear fits of the natural logarithm of fraction $^{32}$P-RNA bound to Hfq versus time.[26,35] The results showed that the dissociation of $^{32}$P-labeled DsrA in the presence of unlabeled ChiX, DsrA, OxyS, McaS, and RybB competitors was biphasic, while the dissociation of IstR1 and SgrS was best fit as a single linear segment (Figure 1B, Table 1). The biphasic dissociation of DsrA and OxyS is in agreement with previous data.[26] ChiX and OxyS were most efficient in inducing the $^{32}$P-DsrA dissociation from Hfq. The rate of the faster dissociation event ($k_{off}^1$) of ChiX was $62 \pm 16 \times 10^{-4}$ s$^{-1}$, while that of OxyS was $72 \pm 14 \times 10^{-4}$ s$^{-1}$. DsrA, McaS, and RybB were less efficient competitors. The unlabeled DsrA induced the dissociation with $k_{off}^1$ value of $46 \pm 15 \times 10^{-4}$ s$^{-1}$, while McaS and RybB sRNAs had $k_{off}^1$ values of $35 \pm 7.9 \times 10^{-4}$ s$^{-1}$, and $29 \pm 8.6 \times 10^{-4}$ s$^{-1}$, respectively. The dissociation rates induced by these five sRNAs are in the same range as observed before for other sRNA molecules.[25,26] On the other hand, the $k_{off}$ values describing dissociation induced by unlabeled IstR1 and SgrS were about 10-fold lower (Table 1). In summary, these data showed that ChiX and OxyS were the most efficient competitors in this assay (Figure 1B, Table 1), DsrA, McaS, and RybB had moderate competition efficiencies, while SgrS and IstR1 were the weakest in this group. These differences in competition *in vitro* (Figure 1B, Table 1) correlate very well with recent *in vivo* data, which showed that OxyS and ChiX sRNAs were most efficient in the competition against positive regulators (DsrA, RprA, ArcZ sRNAs) of Hfq-dependent *rpoS* mRNA translation regulation, while RybB and SgrS were among the least effective competitors.[24] The weaker competition performance of DsrA versus ChiX also agrees with the results of previous *in vivo* studies, which showed that after OxyS overexpression a lower fraction of DsrA remained bound to Hfq as compared to ChiX.[24] Although the *in vivo* competition properties of McaS and IstR1 are not known, the translation regulation by IstR1 is not dependent on Hfq,[38] which suggests it is a poor competitor *in vivo*. Overall, the data showed that the relative properties of sRNAs in competition for Hfq observed *in vitro* (Figure 1B, Table 1) were strikingly consistent with their performance in competition for Hfq observed in *E. coli* cells.[24]

To get more insight into the mechanism of competition, the seven sRNAs were also tested using an equilibrium competition assay at a range of concentrations of unlabeled competitors (Figure 1C, Table 1). Similar assays were used before to study the Hfq binding of Qβ phage RNA,[48] and also of RNA-IN and RNA-OUT.[49] Here, the fraction of 5′-$^{32}$P-labeled DsrA bound to Hfq was monitored to determine the competitor concentration (IC$_{50}$), at which $^{32}$P-DsrA remains 50% bound to Hfq. It is noted that for the most efficient competitors the obtained value of IC$_{50}$ was around 1 nM, which is lower than expected taking into account the 2.2 nM concentration of Hfq (Table 1). This could suggest the ability of certain sRNA molecules to interact with more than one Hfq hexamer simultaneously.[5,50] Alternatively, it could suggest that there is a lower active fraction of Hfq in the conditions of the competition reaction, which could possibly be a result of Hfq aggregation[48,51] or its interactions with the surface of the reaction tubes. Indeed, a control experiment with 0.1 mg/mL

**Table 1. Competition of Unlabeled sRNAs against $^{32}$P-DsrA or $^{32}$P-ChiX sRNA for Binding to the Hfq Protein**[a]

| RNA competitor | rates of dissociation of $^{32}$P-DsrA induced by unlabeled competitor RNAs at 3.75 nM | | 50% competition against $^{32}$P-DsrA, IC$_{50}$ or IC$_{50}^{High}$/IC$_{50}^{Low}$ [nM] | 50% competition against $^{32}$P-ChiX, IC$_{50}$ [nM] |
|---|---|---|---|---|
| | $k_{off}^1$ [s$^{-1}$ × 10$^4$] | $k_{off}^2$ [s$^{-1}$ × 10$^4$] | | |
| ChiX | 62 ± 16 | 7.7 ± 1.4 | 0.84 ± 0.30 | 0.86 ± 0.22 |
| DsrA | 46 ± 15 | 11 ± 3.1 | 0.98 ± 0.48 | 520 ± 170 |
| IstR1 | 2.6 ± 0.53 | s.l. | 1.3 ± 0.9/ 210 ± 80 | >10 000 |
| McaS | 35 ± 7.9 | 6.7 ± 1.6 | 3.5 ± 0.58 | 220 ± 76 |
| OxyS | 72 ± 14 | 13 ± 0.85 | 0.84 ± 0.47 | 33 ± 5.8 |
| RybB | 29 ± 8.6 | 7.7 ± 1.8 | 2.2 ± 0.68 | >10 000 |
| SgrS | 3.8 ± 1.4 | s.l. | 1.2 ± 0.86/ 470 ± 280 | >10 000 |

[a]s.l. - dissociation data were fit as single linear. The numbers are averages of at least three independent experiments.

**Figure 2.** Competition performance of chimeric constructs with transplanted 3′-terminator stem depends on the identity of the 5′ terminal part of the molecules. (A) Structures of chimeric sRNAs with 3′-terminator element transplanted from DsrA sRNA with respective average $k_{off}^1$ and IC$_{50}$ values from at least three independent experiments presented above each structure; (B) the comparison of unlabeled sRNA constructs from (A) in competition against $^{32}$P-DsrA binding to Hfq. The best fits of data presented in the graphs show the IC$_{50}$ values of 1.1 nM for DsrA, 4.6 nM (IC$_{50}^{High}$) and 25 nM (IC$_{50}^{Low}$) for IstR1-DsrA_1, 1.9 nM for McaS-DsrA_1, 6.2 nM for OxyS-DsrA_1, 4.4 nM for RybB-DsrA_1; (C) Structures of chimeric sRNAs with 3′-terminator element transplanted from IstR1 sRNA with respective average $k_{off}^1$ and IC$_{50}$ values from at least three independent experiments presented above each structure; (D) the comparison of competition efficiencies of unlabeled sRNA constructs from (C) against $^{32}$P-DsrA binding to Hfq. The best fits of data show the IC$_{50}$ values of 1.0 nM (IC$_{50}^{High}$) and 290 nM (IC$_{50}^{Low}$) for IstR1, 0.27 nM (IC$_{50}^{High}$) and 70 nM (IC$_{50}^{Low}$) for ChiX-IstR1_1, 0.29 nM (IC$_{50}^{High}$) and 190 nM (IC$_{50}^{Low}$) for DsrA-IstR1_1, 0.44 nM (IC$_{50}^{High}$) and 74 nM (IC$_{50}^{Low}$) for McaS-IstR1_1, 0.3 nM (IC$_{50}^{High}$) and 190 nM (IC$_{50}^{Low}$) for OxyS-IstR1_1. The fitting errors of individual data sets were significantly lower than the errors for the triplicates.

bovine serum albumin in the reaction showed increased $IC_{50}$ values for sRNA competition (data not shown). Importantly, the relative competition performance of sRNAs in this assay is in agreement with the results of the kinetic assay (Figure 1B, Table 1). The data showed that ChiX, OxyS, and DsrA sRNAs were most effective in outcompeting $^{32}$P-DsrA from Hfq with $IC_{50}$ values around 1 nM (Figure 1C, Table 1). RybB and McaS sRNAs were somewhat less effective with $IC_{50}$ between 2 and 4 nM. Interestingly, the weakest competitors IstR1 and SgrS showed a complex picture as the binding curves fit best with a two-site binding competition equation. This could mean that the $^{32}$P-labeled sRNA can bind to Hfq in two different ways (with 1:1 stoichiometry) and that these competitors can only interfere with one of these binding modes. Alternatively, it could mean that more than 1 RNA is bound per Hfq hexamer. For both IstR1 and SgrS sRNAs, the tighter binding event corresponded to $IC_{50}$ value of about 1 nM, while the $IC_{50}$ value of the second one was more than 100-fold weaker. Importantly, IstR1 was not able to completely displace 5′-$^{32}$P-labeled DsrA from its complex with Hfq even at the 2.5 μM concentration (Figure 1C, Table 1). These data are in agreement with previous reports showing that even though IstR1 binds Hfq with similar affinity to other sRNAs,[26] it is very inefficient in competition against other sRNAs for access to this protein.[25,26] This could suggest that Hfq binding by IstR1 involves a different set of contacts than is the case for other sRNAs, which decreases its ability to displace other sRNAs from the complex with Hfq.[25] In agreement with previous data showing that RybB sRNA interacts simultaneously with both the proximal and lateral sites of Hfq,[10] these data could also suggest that the binding of $^{32}$P-DsrA to Hfq also involves two sites, and that SgrS and IstR1 are more efficient in competing against DsrA interactions with Hfq at one of these distinct sites.

As the data showed that ChiX sRNA was the most efficient competitor in both kinds of assays, the competition of unlabeled sRNAs against the $^{32}$P-labeled ChiX in complex with Hfq was also compared (Figure 1D, Table 1). The overall hierarchy of sRNAs was similar to that observed in the competition against $^{32}$P-DsrA, but the differences among them were much larger. As expected, the unlabeled ChiX molecules were most efficient with $IC_{50}$ of approximately 1 nM, and OxyS was the next most efficient sRNA with a $IC_{50}$ value 30-fold weaker than that of unlabeled ChiX. The $IC_{50}$ values of moderate competitors McaS and DsrA were 200-fold and 500-fold weaker, respectively. Finally, RybB, SgrS and IstR1 were very inefficient in the competition assay, and their $IC_{50}$ values were estimated as higher than 10 μM (Figure 1D, Table 1). These data confirm the differences in competition efficiencies of sRNAs (Figure 1B,C, Table 1) and also support the conclusion that ChiX is much more efficient in competition for Hfq than other sRNAs.
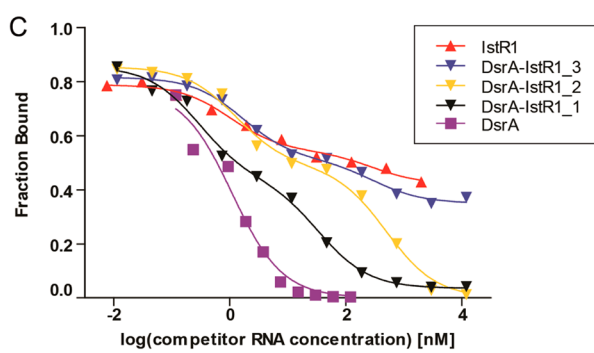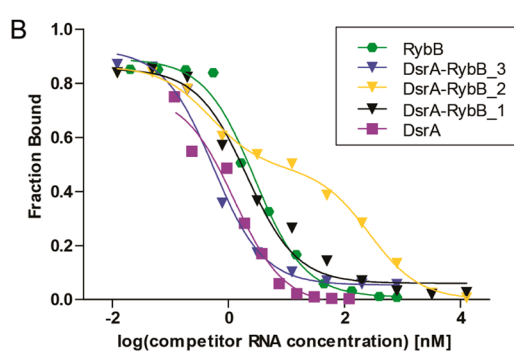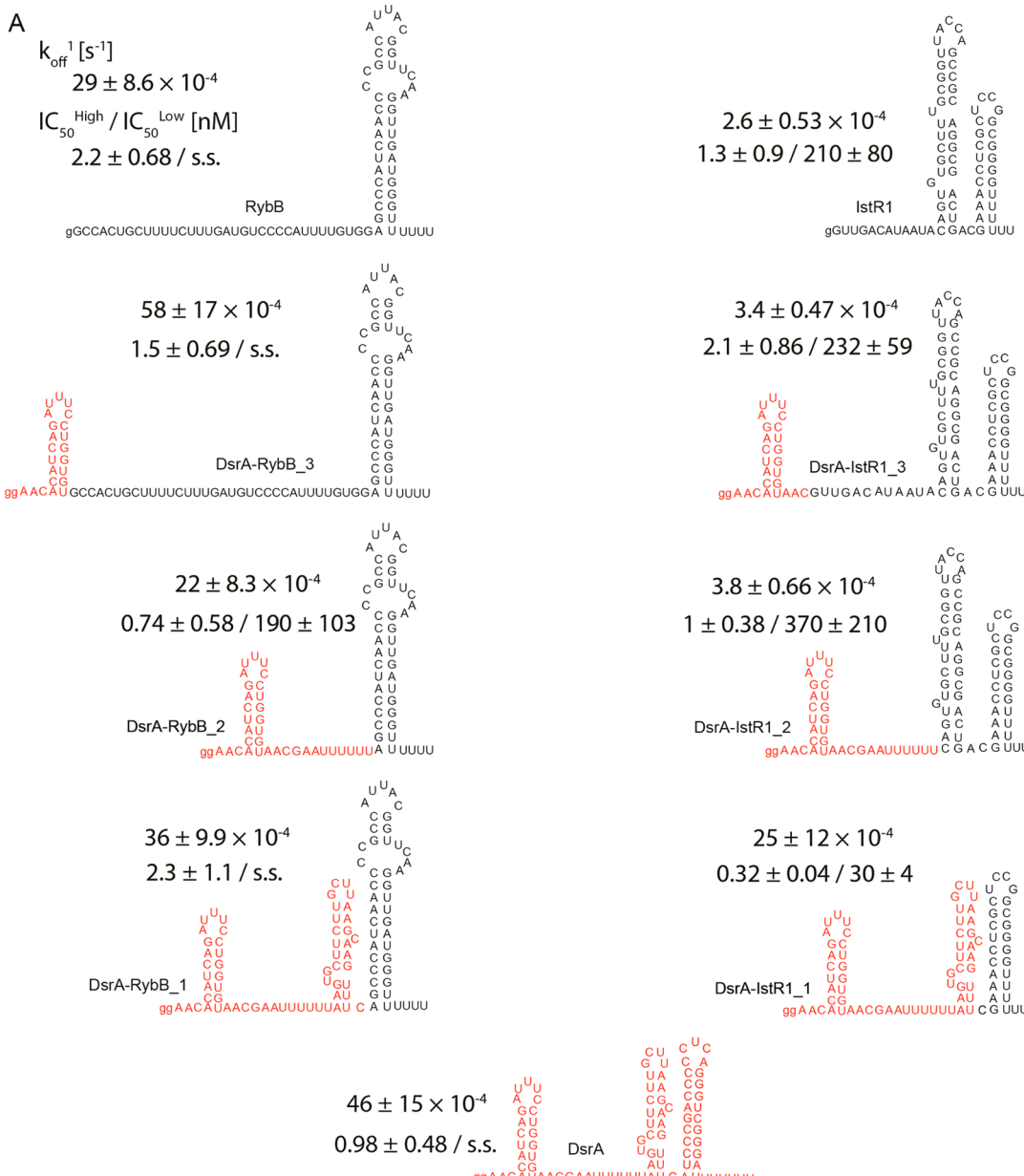
Overall, the relative competition properties of sRNAs shown by the equilibrium assay agree with the results of the kinetic assay (Figure 1B,C, Table 1). Moreover, the equilibrium competition data reveal that the competition by IstR1 and SgrS is more complex than is the case for the other sRNAs. Interestingly, the most efficient competitors ChiX and OxyS have single-stranded regions, which are longer than 25 nt, and are flanked by stem-loop structures on both the 3′ and 5′ termini (Figure 1). On the other hand, the weakest competitors IstR1 and SgrS have shorter single-stranded regions, and lack stem-loops on 5′ termini. The moderately efficient competitors either have a short single-stranded region flanked by stem-loops

on both sides (DsrA, McaS) or have a long single-stranded region without a stem-loop on 5′ side (RybB). This suggests that 5′-terminal stem-loop structures and the presence of long single-stranded regions could be correlated with improved performance of sRNAs in competition for Hfq.

## The 5′ Terminal and Central Regions of sRNAs Modulate Their Performance in Competition for Hfq.

To test if the 5′ terminal and central elements of sRNA structure affect their competition performance two series of sRNA constructs, each series with the same transplanted 3′-terminator structure, were designed (Figure 2). It was previously reported that the 3′-terminal stem-loops with the sequence of uridine residues remaining from Rho-independent terminator were important for SgrS sRNA[13,28] and RybB sRNA[10] binding to Hfq, and were observed to affect competition properties of sRNAs.[26] However, it was not known what is the contribution of the 5′-terminal part of sRNA molecules to their competition performance. To test this, chimeric molecules were designed, which contained the terminator structure of either a strong competitor, DsrA, or a weak competitor, IstR1, which was transplanted at the 3′ end of a set of sRNAs, instead of their natural terminator structures (Figure 2). Chimeric constructs derived from RNA molecules with different properties had been used before to dissect structure and function relationships, for example, in the studies of tRNAs.[52,53] Importantly, the molecules of sRNAs are composed of well-defined structure elements, which enables the design of chimeric constructs without the disruption of individual motifs. The 5′ terminal regions of ChiX, DsrA, IstR1, McaS, OxyS, and RybB molecules were used. However, the "body" of RybB could only be used in the fusion with DsrA terminator, and that of ChiX in the fusion with IstR1 terminator, because the other fusions of these sRNAs would not fold in the same way as natural molecules, as predicted by RNAstructure software.[44] The SgrS sRNA was not tested in these experiments because the full-length molecule is almost 230 nt long, which would make the assessment of the contribution of its 5′-terminal region to the competition performance very complex.

When the constructs with the terminator structures transplanted from a moderately strong competitor DsrA were analyzed, the data showed that all the derived constructs were either similar or weaker in competition for Hfq than the natural DsrA molecule (Figure 2A,B). When the effects of OxyS_DsrA_1 and RybB_DsrA_1 molecules on the dissociation of 5′-$^{32}$P-DsrA from Hfq were measured, they showed a $k_{off}^{1}$ value similar to that of the native DsrA. However, the other two constructs, containing McaS or IstR1 bodies, induced about 2-fold slower dissociation of $^{32}$P-DsrA from the complex with Hfq than the natural DsrA. In agreement with that, the results of the equilibrium competition assay (Figure 2A) showed that $IC_{50}$ values for McaS, OxyS, and RybB derived constructs were 2−3 fold higher than for native DsrA. Moreover, these data showed that the competition curve for IstR1_DsrA_1 molecule had two components, similar to that of natural IstR1. The stronger component had the $IC_{50}$ value similar to that of other constructs and was responsible for most of $^{32}$P-DsrA displacement from the complex, while the weaker component had about 100-fold higher $IC_{50}$ value (Figure 2A,B). Overall, these data showed that the competition performance not only depends on the 3′-terminal stem-loop structures of these RNA constructs, but it is also negatively affected by the 5′-terminal and central regions of these molecules.

**Figure 3.** Chimeric sRNAs combining DsrA sRNA (red) with either RybB sRNA (black, left) or IstR1 sRNA (black, right). (A) Structures of DsrA-RybB and DsrA-IstR1 chimeric sRNAs with respective average $k_{off}^{1}$ and $IC_{50}$ values from at least three independent experiments presented above each structure, s.s. - denotes equilibrium competition data, which were best fit assuming one binding site. (B) Comparison of DsrA-RybB chimeras in competition against $^{32}P$-labeled DsrA sRNA. The best fits of data show the $IC_{50}$ values of 2.8 nM for RybB, 0.55 for DsrA-RybB_3, 0.5 nM ($IC_{50}^{High}$) and 280 nM ($IC_{50}^{Low}$) for DsrA-RybB_2, 2.1 nM for DsrA-RybB_1, and 1.1 nM for DsrA; (C) comparison of DsrA-IstR1 chimeras in competition against $^{32}P$-labeled DsrA sRNA. The best fits of data show the $IC_{50}$ values of 1 nM ($IC_{50}^{High}$) and 290 nM ($IC_{50}^{Low}$) for IstR1, 1.7 nM ($IC_{50}^{High}$) and 300 nM ($IC_{50}^{Low}$) for DsrA-IstR1_3, 1.3 nM ($IC_{50}^{High}$) and 510 nM ($IC_{50}^{Low}$) for DsrA-IstR1_2, 0.29 nM ($IC_{50}^{High}$) and 35 nM ($IC_{50}^{Low}$) for DsrA-IstR1_1, and 1.1 nM for DsrA. The fitting errors of individual data sets were significantly lower than the errors for the triplicates.

When the constructs containing the terminator structure from the weak competitor IstR1 were tested, the data showed that all the fusions were better competitors than the native IstR1 molecule (Figure 2C,D). It was especially evident when the kinetic assay was used because the $k_{off}^1$ values for all the constructs were about 10-fold faster than for the natural IstR1 molecule (Figure 2C). When competition was compared using the equilibrium assay it appeared that the competition curves for all the fusions had two components (Figure 2D), as similarly observed for natural IstR1 (Figure 1, Table 1). Importantly, all the fusion constructs were more efficient in competition than natural IstR1. The $IC_{50}$ values for both components of the competition curve were 2−3 times lower than in the case of natural IstR1 (Figure 2C). Moreover, the fusions differed in the extent of displacement of $^{32}$P-DsrA from the complex. When the fusions containing ChiX, McaS, and DsrA bodies were used, $^{32}$P-DsrA was almost completely displaced from the complex at the highest 10 $\mu$M concentration, with 10% or less of DsrA remaining bound. However, when the fusions containing OxyS body were examined more than 20% of initial fraction bound remained in the complex, while for the natural IstR1 used as a competitor as much as 50% of the initial complex remained at this concentration (Figure 2D). This could suggest that the 3′-terminal motif with a short unpaired sequence of two uridines derived from IstR1 confers on the chimeric constructs the inability to efficiently compete against $^{32}$P-DsrA in complex with Hfq. However, these data clearly showed that even though all the constructs were negatively affected by the presence of the 3′-terminator structure from the weak competitor IstR1, they were still much more efficient in competition than the natural IstR1 molecule. This shows the important role of the 5′-terminal and central parts of the sRNA body in determining its competition performance.

**Influence of Structure Elements from the 5′-Terminal and Central Part of DsrA on the Competition Performance of Chimeric Constructs Depends on Their Structural Context.** To better understand how the individual structural features present in the 5′-terminal and central parts of sRNA molecules affect competition, we designed two series of chimeric constructs, each composed of a sequence of a weaker competitor, either RybB or IstR1, and an increasing amount of the sequence of a good competitor DsrA (Figure 3). To test if the individual structure elements of sRNAs remain intact after transplanting them into chimeric constructs, RNA structure probing with RNases T2 and S1 was used (Supplemental Figures 2 and 3, Supporting Information). The comparison of cleavage patterns characterizing individual structure elements of natural DsrA and RybB with those of chimeric molecules showed that the probing signatures of apical loops and single-stranded regions of these sRNAs were preserved in the chimeric RNAs (Supplemental Figure 2). Similarly, when the probing patterns of IstR1 and DsrA were compared with the corresponding chimeras, the data showed that the individual structure elements were retained. Because the RNase T2 probing of the 5′-single-stranded region of IstR1 required a shorter reaction time than DsrA-IstR1_3 chimera and other molecules, it appears that the single-stranded region of IstR1 is stabilized by the transplantation of the 5′-terminal stem-loop from DsrA onto IstR1 (Supplemental Figure 3). It remains possible that single-stranded regions of sRNAs could be involved in transient interactions affecting the structural dynamics of sRNA molecules,[54] which could be important for their competition performance. However, such unstable interactions were not detected by probing with RNases. Overall, the data show that the secondary structure modules of DsrA, RybB, and IstR1 sRNAs remain intact after transplanting them into these two series of chimeric constructs (Figure 3, Supplemental Figures 2 and 3).

Both dissociation and equilibrium data showed that when the 5′-terminal stem-loop from DsrA was transplanted onto the 5′ end of RybB, the resulting chimera (DsrA-RybB_3) was as good in competition as DsrA and much better than natural RybB (Figure 3). However, when the single-stranded region of RybB was replaced with that from DsrA (DsrA-RybB_2) the chimera became less efficient than DsrA-RybB_3 with $k_{off}^1$ value similar to that of RybB and 2-fold slower than for DsrA-RybB_3. The poor competition performance of the DsrA-RybB_2 chimera was even more evident in the equilibrium data, which showed that to achieve 50% displacement of $^{32}$P-DsrA the concentration of unlabeled DsrA-RybB_2 needed to be around 100 nM (Figure 3A,B). Finally, the whole 5′ region of DsrA was attached to the terminator structure of RybB resulting in the construct DsrA-RybB_1 (Figure 3A). In this case, the $k_{off}^1$ value was not significantly different from those of RybB or DsrA; however, the performance of this chimera was much better in the equilibrium competition experiment as the displacement of 50% of $^{32}$P-DsrA required only around 2 nM concentration of this chimera. In summary, these data showed that the addition of the stem-loop on the 5′end of the 34-nt long single-stranded region of RybB made it a much better competitor. However, when this long region was replaced with the 3-times shorter, 12-nt long single-stranded region derived from DsrA the improvement in the competition performance was lost.

When the chimeras composed of IstR1 and increasing amounts of DsrA sequence were assayed, the competition efficiency improved only when the whole 5′-terminal and central part of DsrA sequence was introduced into the construct (Figure 3A). Unlike in the case of RybB chimeras, the addition of the 5′-terminal stem from DsrA (DsrA-IstR1_3) did not improve the performance in the dissociation or equilibrium assays. Also when the IstR1 single-stranded sequence was replaced with that from DsrA (DsrA-IstR1_2), the competition properties did not change in comparison to DsrA-IstR1_3. Finally, the construct with the complete DsrA body fused to the IstR1 terminator (DsrA-IstR1_1, the same as used in the terminator transplant experiments) induced a 10-fold faster dissociation of $^{32}$P-DsrA from Hfq, and had a 4-fold lower value of $IC_{50}$ for the tighter binding event (Figures 2 and 3), in comparison to the other chimeras and natural IstR1. This shows that in the context of IstR1 structure the addition of the 5′-terminal stem-loop from DsrA was not sufficient to markedly improve the performance, and the whole 5′-terminal and central part of the DsrA molecule was necessary to compensate for the detrimental effect of the 3′-terminator structure from IstR1.

Overall, both series of experiments showed that the internal structural elements of sRNA bodies affected their competition performance. The data indicate that a 5′ terminal stem-loop and a more than 30-nt long single-stranded region are the positive determinants of competition for Hfq in the context of a RybB molecule. However, when the 5′ terminal stem-loop from DsrA was attached to the short 12-nt single-stranded region of IstR1, it had only a small influence, which suggests that the

Table 2. Equilibrium Binding of RNAs to the Hfq Protein and Its Variants with Mutations in Proximal, Distal, or Rim Surfaces[a]

| | $K_d$ (nM) | | | |
|---|---|---|---|---|
| RNA | wild type Hfq | Hfq (Y25D) | Hfq (K56A) | Hfq (R16A) |
| ChiX | 0.21 ± 0.13 | 0.23 ± 0.1 | 0.44 ± 0.18 | 0.21 ± 0.09 |
| DsrA | 0.54 ± 0.21[b] | 0.4 ± 0.14 | 6.2 ± 0.51 | 0.58 ± 0.21 |
| IstR1 | 0.7 ± 0.34[b] | 0.77 ± 0.28[b] | 150 ± 66[b] | 64 ± 33 |
| McaS | 0.31 ± 0.12 | 0.31 ± 0.1 | 9 ± 2.6 | 0.61 ± 0.37 |
| OxyS | 0.26 ± 0.072[b] | 0.48 ± 0.22 | 8 ± 2.7 | 0.5 ± 0.05 |
| RybB | 0.34 ± 0.09 | 0.52 ± 0.19 | 11 ± 0.65 | 1.2 ± 0.54 |
| SgrS | 0.45 ± 0.15 | 0.4 ± 0.01 | 8.4 ± 2.8 | 0.42 ± 0.04 |
| McaS_U3 | 0.85 ± 0.5 | 0.13 ± 0.06 | 8.1 ± 0.51 | 11 ± 1.3 |
| McaS_U1 | 2 ± 0.56 | 0.21 ± 0.16 | 19 ± 5.2 | 31 ± 14 |
| DsrA_U1 | 0.29 ± 0.14 | n.m.[c] | n.m. | 26 ± 11 |
| RybB_U1 | 0.19 ± 0.06 | n.m. | n.m. | 32 ± 17 |
| OxyS_U4 | 0.22 ± 0.12 | n.m. | n.m. | 1.8 ± 0.3 |
| ChiX_U3 | 0.48 ± 0.11 | 0.36 ± 0.07 | 0.58 ± 0.15 | 0.44 ± 0.16 |
| ChiX_U0 | 0.72 ± 0.11 | 1.1 ± 0.54 | 1.6 ± 0.51 | 0.62 ± 0.25 |
| ChiX-M1 | 0.23 ± 0.13 | 0.21 ± 0.09 | 1.4 ± 0.42 | 0.21 ± 0.08 |
| ChiX-M2 | 0.24 ± 0.12 | 0.19 ± 0.09 | 2.8 ± 1.1 | 0.23 ± 0.06 |
| ChiX-M3 | 0.12 ± 0.03 | 0.32 ± 0.05 | 0.61 ± 0.21 | 0.25 ± 0.03 |
| ChiX-M4 | 0.26 ± 0.09 | 1 ± 0.28 | 0.98 ± 0.25 | 0.35 ± 0.15 |

[a]The numbers are averages of at least three independent experiments. [b]$K_d$ values from ref 26 where full-length DsrA was named DsrA-U7, and full-length OxyS was named OxyS-U8. [c]n.m. − not measured.
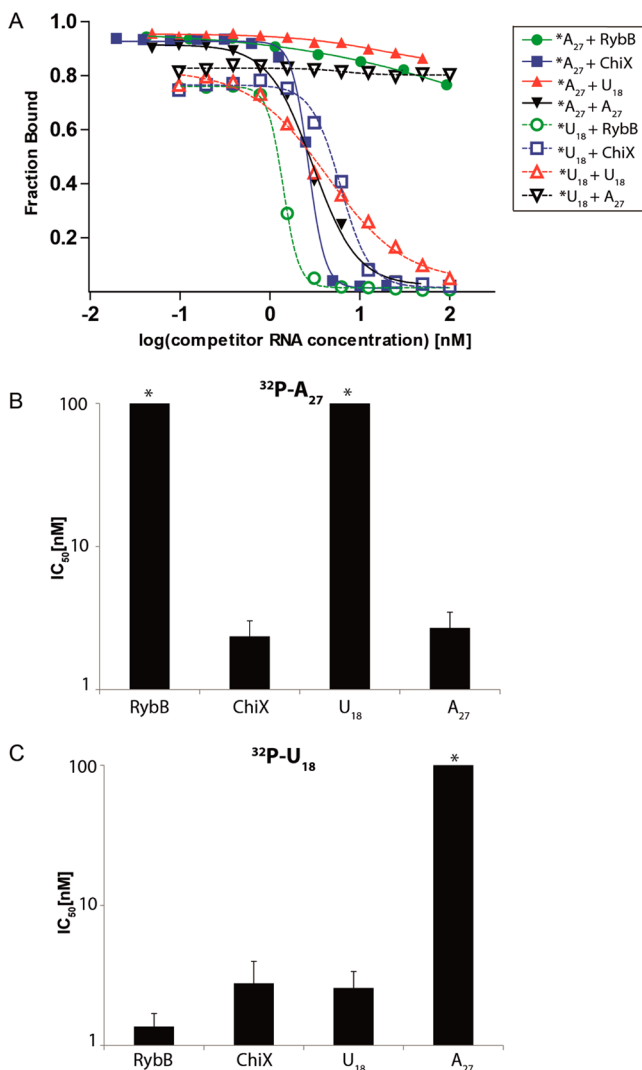
exact effect of this motif depends on the surrounding structure elements.

**Differential Binding of sRNAs to the Proximal, Distal, and Rim Sites of Hfq.** To test if differences in competition between sRNAs could be explained by their different interactions with Hfq, their affinities to the variants of E. coli Hfq protein containing mutations in the proximal, distal, or rim RNA binding sites were compared (Table 2). The equilibrium binding of ^{32}P-labeled sRNAs to Hfq was measured using a filter retention assay. The Hfq variants with mutation Y25D in the distal site,[8] K56A in the proximal site,[8] or R16A on the rim of Hfq[10] were used. All sRNAs showed similar, sub-nanomolar affinities to the wild type Hfq and the distal face Y25D mutant (Table 2), which was expected based on previous results.[26] However, when the binding to the proximal face K56A mutant was tested six out of seven sRNAs had at least 15-fold weaker binding. On the other hand, this mutation was not detrimental for ChiX sRNA binding (Table 2). Additionally, when the binding to the Hfq variant with the rim surface R16A mutation was measured, the data showed that its effect was very small for all sRNAs except IstR1, which showed more than 80-fold weaker binding to this mutant than to wt Hfq (Table 2). Overall, the equilibrium binding data showed that DsrA, McaS, OxyS, RybB, and SgrS had the same sensitivity toward mutations in the three binding sites on Hfq (Table 2). However, IstR1 was more sensitive than others to the rim R16A mutation, while the binding of ChiX sRNA was not affected by any of the individually tested mutations.

To better understand how the sites on Hfq are involved in the interactions with these sRNAs, the ChiX, DsrA, McaS, OxyS, and RybB derivatives with truncated oligoU tails were compared in binding to Hfq (Table 2). It was recently proposed that the 3′-terminal oligoU "tail" of RybB binds strongly to the proximal face, and the interactions of RybB with another site on the rim of Hfq could only be detected after the binding of the oligoU "tail" was weakened by modification.[10] To test if this could also be the case for other sRNAs, two mutants of McaS sRNA with truncations of the 3′ uridine "tail"

were designed, one of which had three uridines (McaS_U3) and the other one uridine (McaS_U1) remaining. The data showed that the binding of both McaS_U3 and McaS_U1 to wt Hfq, Hfq Y25D, and Hfq K56A had similar affinities as that of full-length McaS. However, the binding of McaS_U3 and McaS_U1 to Hfq R16A was 18-fold and 50-fold, respectively, weaker than that of full-length McaS. Similarly, when the binding of DsrA_U1, RybB_U1, and OxyS_U4 constructs to wt Hfq was compared (Table 2), all showed unaffected binding. However, DsrA_U1 and RybB_U1 exhibited, respectively, 40-fold, and 25-fold weaker binding to the R16A mutant than the full-length DsrA and RybB molecules, while OxyS_U4, which had four uridines remaining in the "tail", had 3-fold weaker binding to this Hfq mutant than the full-length OxyS. Finally, two mutants of ChiX with truncations of the 3′-terminal uridine "tail" were designed. The ChiX_U3 mutant had three out of seven uridines remaining at the 3′ end, while the ChiX_U0 mutant had the uridine "tail" completely removed. The data showed that the absence of four 3′-terminal uridines in ChiX-U3 had a very weak effect on its binding to Hfq and its mutants, and even the complete absence of the 3′ terminal uridines in ChiX_U0 had a quite small and uniform, up to 3-fold, detrimental effect on its binding to wt Hfq and all three mutants (Table 2). This suggests that after removal of the 3′ uridine "tail" other strong contacts remain, which firmly anchor ChiX on the Hfq protein. Overall, these data suggest that the affinity of DsrA, McaS, OxyS, and RybB to Hfq has a strong component dependent on the binding to the rim site, the effect of which is unmasked when the binding to the proximal site is abolished by removing the 3′-terminal uridine tail. However, these data also underline that the mode of ChiX binding to Hfq is different than that of other sRNAs.

**Interactions of ChiX sRNA with Hfq Involve Binding to the Opposite Faces of the Hfq Ring.** To test if ChiX sRNA could interact with the opposite surfaces of Hfq, we monitored the effect of unlabeled ChiX concentration on the binding of ^{32}P-labeled oligoriboadenylate ($A_{27}$) or oligoribouridylate ($U_{18}$) to Hfq (Figure 4). Oligoadenylates bind to a circular site on the
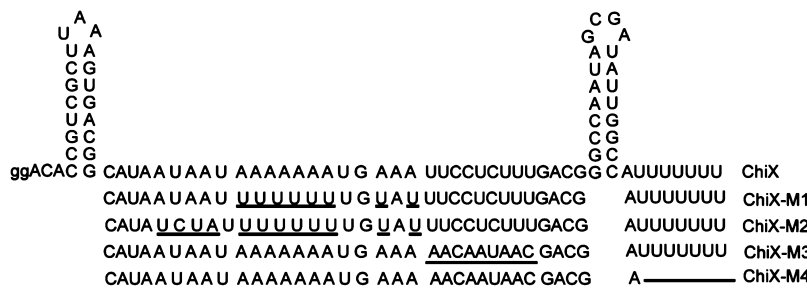
**Figure 4.** ChiX sRNA efficiently outcompetes both $A_{27}$ and $U_{18}$ from the complex with Hfq. (A) The plot of $^{32}P$-labeled $A_{27}$ and $^{32}P$-labeled $U_{18}$ (denoted as $*A_{27}$ and $*U_{18}$ in the plot legend) binding to Hfq in the presence of indicated unlabeled RNAs. The best fits of data to the competition equation with Hill coefficient ($n$) show the IC$_{50}$ values of $^{32}P$-$A_{27}$ as 2.7 nM ($n = -4.7$) for ChiX, and 3.0 nM ($n = -1.8$) for $A_{27}$. IC$_{50}$ values for unlabeled RybB and $U_{18}$ were estimated as higher than 100 nM. The best fits of data to the competition equation with Hill coefficient show the IC$_{50}$ values of $^{32}P$-$U_{18}$ as 1.4 nM ($n = -4.9$) for RybB, 6.1 nM ($n = -2.7$) for ChiX, and 4.3 nM ($n = -1.0$) for $U_{18}$. The IC$_{50}$ value for unlabeled $A_{27}$ was estimated as higher than 100 nM. (B) The average IC$_{50}$ values for the competition of unlabeled RNAs against $^{32}P$-$A_{27}$. The average values of Hill coefficients are $-4.8 \pm 1.2$ for ChiX and $-1.7 \pm 0.28$ for $A_{27}$. (C) The average IC$_{50}$ values for the competition of indicated RNAs against $^{32}P$ labeled $U_{18}$. The average values of Hill coefficients are $-4.2 \pm 0.62$ for RybB, $-3.6 \pm 0.47$ for ChiX and $-1.2 \pm 0.13$ for $U_{18}$. Bars marked with * correspond to IC$_{50}$ values, which were estimated as higher than 100 nM. All experiments were performed at least in triplicate. The fitting errors of individual data sets were significantly lower than the errors for the triplicates.

distal face of Hfq,[8,9] while oligouridylates bind around the central pore of Hfq ring on the proximal face.[12] As expected, the unlabeled $A_{27}$ prevented the binding of $^{32}P$-labeled $A_{27}$, but did not affect the binding of $^{32}P$-labeled $U_{18}$ (Figure 4A,B). Conversely, the unlabeled $U_{18}$ prevented the binding of $^{32}P$-labeled $U_{18}$, but did not affect the binding of $^{32}P$-labeled $A_{27}$.

These data confirm that $A_{27}$ binding is specific to the distal face, and $U_{18}$ to the proximal face of Hfq in the conditions of this experiment. Importantly, when unlabeled RybB sRNA was tested it prevented the binding of $^{32}P$-labeled $U_{18}$, but did not markedly affect the binding of $^{32}P$-labeled $A_{27}$, which is consistent with its exclusive binding to the proximal and rim surfaces of Hfq.[10] However, when unlabeled ChiX was tested it very efficiently prevented the binding of both $A_{27}$ and $U_{18}$ to Hfq (Figure 4). This shows that ChiX sRNA strongly binds both to the proximal and the distal face of Hfq.

To explain why ChiX sRNA is capable of binding to both faces of Hfq, two mutants of this sRNA were analyzed, in which multiple adenosines in the central, single-stranded region were substituted to uridines (Figure 5, Table 2). The characteristic feature of ChiX is the internal 34-nt long single-stranded region. It contains 15 adenosine residues in the 5′-terminal portion of this region, which includes a perfect $(AAN)_4$ motif, or an $(AAN)_6$ motif with a single mismatch, such as sequences identified as strong Hfq binding sites in mRNAs.[55] In the first mutant (ChiX-M1) nine of those adenosines were replaced with uridines (Figure 5). The predicted secondary structure of ChiX-M1 remained the same, as judged by RNAstructure.[44] The data showed that the mutations did not change the affinity of ChiX to wt Hfq or its Y25A and R16A variants defective in the binding to the distal or rim sites (Table 2). However, the binding of this molecule to the Hfq variant with proximal site K56A mutation was 3-times weaker than the binding of wt ChiX. To further analyze this effect another mutant (ChiX-M2) was designed, which had additional three adenosines replaced, resulting in 13 out of 15 adenosines in the 5′ portion of the single-stranded region substituted with uridines (Figure 5). This mutant had a further 2-fold effect on Hfq K56A variant binding (6-fold in comparison to wt ChiX), while the affinity to wt Hfq or the other two Hfq variants was not affected (Table 2). This could suggest that the substitution of adenosines in the central region with uridines makes the Hfq binding of this sRNA dependent on the uridine-specific proximal site, which explains why the K56A mutation is more detrimental for ChiX-M2 binding. Moreover, these data suggest that the unique, highly adenosine enriched single-stranded region of ChiX plays an important role in its binding to Hfq, presumably via interactions with the distal site.

To further understand the unique properties of ChiX in binding to Hfq, two additional mutants of this sRNA were analyzed (Figure 5, Table 2). In one of the mutants (ChiX-M3), several uridines in the central region were substituted to adenosines, while the other mutant (ChiX-M4) additionally had the 3′-terminal uridine tail removed (Figure 5). These mutations are not expected to alter the secondary structure of ChiX because the structure probing of ChiX-M3 in comparison to wt ChiX showed the same cleavage patterns of both RNAs induced by RNases T2 and S1 (Supplemental Figure 4, Supporting Information). The binding affinity of ChiX-M3 to Hfq and its mutants was not affected (Table 2). However, the ChiX-M4 mutant was sensitive to the distal face mutation Y25D, and the proximal mutation K56A, similar to the mutant ChiX-U0 (Table 2). The sensitivity to Y25D mutation suggests the binding to the distal face was the major contributor of ChiX-M4 binding to Hfq, consistent with the removal of most of the uridines from the sRNA. This made ChiX-M4 dependent on the contacts made by adenosine residues, which are specific for the distal face. It remains unclear why the increased sensitivity to the K56A mutation on the proximal face was also

**Figure 5.** Mutants of ChiX sRNA. Substitution changes are underlined in the sequence of the single-stranded regions below the ChiX structure. Deletion of all uridines from the 3′ terminal tail of ChiX_M4 mutant is marked by a line. The stem-loops of ChiX remained unmodified in all mutants.

observed, which would suggest that residual binding to the proximal face remained even after the extensive changes, possibly resulting from interactions with the AC-rich region in the single-stranded region of the mutated molecule. Overall, these data suggest that ChiX sRNA has a unique mode of binding to Hfq, which involves simultaneous binding to several sites. The ability to form contacts with several sites on Hfq explains its superior competition performance, as it allows it to bind to Hfq already in complex with another sRNA, presumably facilitating the displacement of the resident sRNA.

## DISCUSSION

The chaperone protein Hfq interacts with many RNAs in the bacterial cell, which decreases the pool of free Hfq available for sRNA binding, and makes the concentration of Hfq limiting for sRNA-dependent regulation.[23] This suggests that the regulatory RNAs can only access this protein after other RNAs are displaced from the complex. Recent *in vitro* data showed that sRNAs have an active role in this displacement,[25] the rates of which depend on both the concentration and the identities of competing sRNAs.[25,26] The *in vivo* competition among sRNAs for Hfq was suggested when unpartnered sRNAs or mRNAs were overexpressed in *E. coli* cells leading to decreased translation regulation by other sRNAs,[23] and also in separate experiments, in which ArcZ sRNA was overexpressed in *Salmonella* cells resulting in differential changes in amounts of other sRNAs that immunoprecipitated with Hfq.[56] Moreover, a very detailed recent analysis showed that there is a hierarchy of sRNAs in competition for Hfq *in vivo*, which was deduced by monitoring the translation of *rpoS* mRNA after overexpressing competitor sRNAs.[24] The data presented here (Figure 1, Table 1) show that the relative efficiencies of sRNAs in competition for Hfq determined *in vitro* are consistent with those observed *in vivo*.[24]

Such differences among sRNAs in their competition performance are quite surprising because recent data showed an important role of Rho-independent terminator stem-loop with an adjacent uridine-rich sequence in the binding of sRNAs to Hfq.[13,28] This 3′-terminal structure is present in all *trans*-encoded sRNAs, which could imply their uniform properties in competition for access to Hfq. As the opposite is evident from both *in vitro*[25,26] and *in vivo*[23,24] data, it suggests that other parts of sRNA molecules play essential roles in determining the differential properties of sRNAs leading to the hierarchy among sRNAs in competition for Hfq. Such differences among sRNAs in their ability to gain access to the Hfq hexamer, which is already bound by another sRNA, could be important for fine-tuning of translation regulation networks,[56,57] for example,

when bacterial cells respond to multiple stresses occurring simultaneously.

The competition data presented here (Figure 2) and reported previously[26] confirm that the length of the unpaired sequence of 3′ terminal uridines remaining from the *rho*-independent terminator affects the competition performance. The role of this element in competition is consistent with its role in Hfq binding and translation regulation by SgrS sRNA.[13,28] Indeed, when the 3′-terminator structure from DsrA sRNA including the 7-uridine "tail" was introduced into the sequences of several different sRNAs, it conferred on them improved competition efficiency, while that from IstR1, which has only two unpaired uridines at the 3′ terminus, was detrimental for their performance (Figure 2). The role of 3′-terminal uridines in competition is in agreement with previous data, which showed that the OxyS molecule without 3′-terminal uridines was a very inefficient competitor,[26] while the full-length molecule with the complete string of eight uridines studied here (Figure 1, Table 1) was among the most efficient competitors, in agreement with *in vivo* data.[24] On the other hand, the data presented here showed (Figure 1, Table 1) that the 5′-terminally truncated SgrS molecule, the same as studied before,[13,28] which had the optimal length of eight uridines in its 3′ terminal "tail" was quite inefficient in competition, in agreement with *in vivo* data.[24] Hence, despite the optimal 8-uridine "tail" length SgrS had a similar level of competition performance as IstR1, which had only two unpaired uridines in the 3′-"tail" (Figure 1, Table 1). This suggests that other structural elements in the sRNA "body", outside of the 3′-terminal region, modulate the influence of the 3′ terminal oligouridine "tail" on the sRNA performance in competition.

The structural motifs present in the 5′ terminal regions of sRNA molecules are important for their competition efficiency, but their roles depend on the structural contexts, in which these motifs are located in an sRNA molecule. Indeed, it was previously shown that the 5′-terminal stem-loop was important for DsrA binding to Hfq.[29] The data presented here show that when this element derived from DsrA sRNA was transplanted onto the 5′ end of RybB sRNA it improved its competition performance (Figures 1 and 3, Table 1). On the other hand, when it was added onto IstR1 it did not improve the efficiency of competition, which suggests that its role could be dependent on the sequence context. The RybB molecule has a more than 25-nt long single-stranded region, while IstR1 has only a short stretch of unpaired residues (Figure 1). Possibly, the 5′ stem-loop could affect competition by stabilizing the long single-stranded region of RybB in a conformation enabling it to form better contacts with Hfq. Another structural element important for competition could be a long single-stranded region present

in several sRNAs (Figure 1). In ChiX sRNA, which is the most efficient competitor studied here (Figure 1, Table 1), this single-stranded region has asymmetric localization of adenosine and uridine residues, with adenosines located mostly in the 5′ terminal part of this sequence, and uridines located mostly in the 3′ part. As this single-stranded region in ChiX is 35-nt long it could wrap around the rim of the Hfq ring to allow the adenosine-rich and uridine-rich sequences of the molecule to contact the opposite faces of Hfq. Overall, these data suggest that sRNAs use different structural motifs to modulate their ability to gain access to the Hfq protein in competition with other RNA molecules.

The efficiency of an sRNA in getting access to Hfq may depend on its ability to bind to several sites on this protein. The differences in the contacts formed by sRNAs with these individual sites could affect their ability to displace other sRNAs from this protein, for example, when the two competing sRNAs use different sets of contacts with Hfq for binding. It was recently reported that the binding of several sRNAs, including DsrA and OxyS, was uniformly dependent on the binding to the proximal face of Hfq.[26] Indeed, also the data presented here (Table 2) show that the binding of six of the seven studied sRNAs was dependent on the proximal face mutation. However, the data on Hfq binding by truncated sRNA constructs (Table 2) suggest that DsrA, McaS, OxyS, and RybB interact with Hfq also at the rim site, in agreement with a recent report showing that RybB sRNA interacts simultaneously with the proximal and rim sites of Hfq.[10] The mode of ChiX interactions with Hfq is unique because it binds the opposite—proximal and distal—faces of the Hfq ring (Figure 4, Table 2). The differential interactions of sRNAs with Hfq are supported by recent *in vivo* data, which showed that the regulation of translation by sRNAs DsrA, McaS, and ChiX was differently dependent on mutations in the RNA binding sites of the Hfq protein.[22] In other studies, RprA sRNA was shown by mutagenesis[58] and by SAXS structure analysis[31] to interact with the distal face of Hfq. However, the RprA construct used in the latter studies had a truncated 3′ uridine "tail", which would presumably make it less likely to interact with the proximal site. Also, when the OxyS sRNA molecule was mutated to introduce an artificial $(AAN)_7$ repeat sequence it made its binding to Hfq more dependent on the distal face.[26] The studies of ChiX mutants presented here (Figure 4, Table 2) suggest that the long adenosine-rich stretch in the 5′ portion of the central single-stranded region of ChiX plays an essential role in the distal face binding by ChiX. To our knowledge, this is the only example of a natural sRNA binding to the distal face of Hfq using an $(AAN)_4$ repeat, which is considered a strong Hfq binding site in mRNA molecules.[4,55] Hence, the unique structure and sequence features of ChiX enable it to be a very efficient competitor for access to Hfq *in vitro* (Table 2) and *in vivo*,[24] which could also explain its exceptional *in vivo* stability allowing it to regulate multiple mRNA targets.[40]

The differences among sRNAs in the way they interact with Hfq could be important for the annealing of sRNAs to their mRNA targets. Recent *in vivo* data using *E. coli* Hfq mutants showed that different sRNA–mRNA pairs are differently dependent on Hfq mutations for efficient translation regulation.[22] For example, negative regulation of *chip* mRNA by ChiX sRNA was strongly dependent on several proximal and rim mutations, and partially on the distal face mutations, while the positive regulation of *rpoS* mRNA by DsrA sRNA was dependent only on the K56A mutation on the proximal side

and the Y25A mutation on the distal side.[22] It has been proposed that Hfq mediates the annealing of sRNAs to mRNAs by binding the former on the proximal face and the latter on the distal one.[9,12] However, in agreement with the data presented here (Figure 4), several recent examples show that both mRNAs[19] and sRNAs[10,31] can interact with more than one site on Hfq, which could affect the access of these RNAs to Hfq and the efficiency of sRNA annealing to mRNAs. It is also worth noting that the specificity of sRNAs and mRNAs toward the binding sites on Hfq may differ among bacterial species.[59,60]

The diversity of sRNA structural properties provides an important way of tuning their ability to access the chaperone protein Hfq, and consequently exert their effect on translation. The data presented here show that besides the minimal Hfq binding motif composed of the terminator stem-loop accompanied by U-rich sequences, also the 5′-terminal and central regions of sRNA body make important contributions to the sRNA success in competition for Hfq. However, it is clear that each sRNA uses a different composition of sequence and structure motifs to tune its interaction with Hfq for optimal translation regulation, leading to a hierarchy among sRNAs in the competition for this protein. Overall, recent data paint a complex picture of interactions between sRNAs and Hfq, which are dependent on multiple RNA binding sites on the surface of Hfq, and on the individual structural features of sRNAs, some of which are shared among many sRNAs, while others are idiosyncratic.

## ■ ASSOCIATED CONTENT

**ⓢ Supporting Information**

Four supplemental figures of RNA secondary structure probing are available free of charge via the Internet at http://pubs.acs.org.

## ■ AUTHOR INFORMATION

**Corresponding Author**
*Phone: +48-61-8295906. Fax: +4861 829-5949. E-mail: mol@amu.edu.pl.

**Notes**
The authors declare no competing financial interest.

## ■ ACKNOWLEDGMENTS

## ■ REFERENCES

(1) Waters, L. S., and Storz, G. (2009) Regulatory RNAs in bacteria. *Cell* 136, 615−628.

(2) Gottesman, S., and Storz, G. (2011) Bacterial small RNA regulators: versatile roles and rapidly evolving variations. *Cold Spring Harbor Perspect. Biol.* 3, a003798.

(3) Romby, P., Vandenesch, F., and Wagner, E. G. (2006) The role of RNAs in the regulation of virulence-gene expression. *Curr. Opin. Microbiol.* 9, 229−236.

(4) Tree, J. J., Granneman, S., McAteer, S. P., Tollervey, D., and Gally, D. L. (2014) Identification of Bacteriophage-Encoded Anti-sRNAs in Pathogenic *Escherichia coli*. *Mol. Cell 55*, 199−213.

(5) Zhang, A., Wassarman, K. M., Ortega, J., Steven, A. C., and Storz, G. (2002) The Sm-like Hfq protein increases OxyS RNA interaction with target mRNAs. *Mol. Cell 9*, 11−22.

(6) Soper, T., Mandin, P., Majdalani, N., Gottesman, S., and Woodson, S. A. (2010) Positive regulation by small RNAs and the role of Hfq. *Proc. Natl. Acad. Sci. U.S.A. 107*, 9602−9607.

(7) Schumacher, M. A., Pearson, R. F., Møller, T., Valentin-Hansen, P., and Brennan, R. G. (2002) Structures of the pleiotropic translational regulator Hfq and an Hfq-RNA complex: a bacterial Sm-like protein. *EMBO J. 21*, 3546−3556.

(8) Mikulecky, P. J., Kaw, M. K., Brescia, C. C., Takach, J. C., Sledjeski, D. D., and Feig, A. L. (2004) Escherichia coli Hfq has distinct interaction surfaces for DsrA, rpoS and poly(A) RNAs. *Nat. Struct Mol. Biol. 11*, 1206−1214.

(9) Link, T. M., Valentin-Hansen, P., and Brennan, R. G. (2009) Structure of Escherichia coli Hfq bound to polyriboadenylate RNA. *Proc. Natl. Acad. Sci. U. S. A. 106*, 19292−19297.

(10) Sauer, E., Schmidt, S., and Weichenrieder, O. (2012) Small RNA binding to the lateral surface of Hfq hexamers and structural rearrangements upon mRNA target recognition. *Proc. Natl. Acad. Sci. U. S. A. 109*, 9396−9401.

(11) Sun, X., and Wartell, R. M. (2006) Escherichia coli Hfq binds A18 and DsrA domain II with similar 2:1 Hfq6/RNA stoichiometry using different surface sites. *Biochemistry 45*, 4875−4887.

(12) Sauer, E., and Weichenrieder, O. (2011) Structural basis for RNA 3′-end recognition by Hfq. *Proc. Natl. Acad. Sci. U. S. A. 108*, 13065−13070.

(13) Otaka, H., Ishikawa, H., Morita, T., and Aiba, H. (2011) PolyU tail of rho-independent terminator of bacterial small RNAs is essential for Hfq action. *Proc. Natl. Acad. Sci. U. S. A. 108*, 13059−13064.

(14) de Haseth, P. L., and Uhlenbeck, O. C. (1980) Interaction of Escherichia coli host factor protein with oligoriboadenylates. *Biochemistry 19*, 6138−6146.

(15) Panja, S., and Woodson, S. A. (2012) Hfq proximity and orientation controls RNA annealing. *Nucleic Acids Res. 40*, 8690−8697.

(16) Peng, Y., Soper, T. J., and Woodson, S. A. (2014) Positional effects of AAN motifs in rpoS regulation by sRNAs and Hfq. *J. Mol. Biol. 426*, 275−285.

(17) Salim, N. N., Faner, M. A., Philip, J. A., and Feig, A. L. (2012) Requirement of upstream Hfq-binding (ARN)x elements in glmS and the Hfq C-terminal region for GlmS upregulation by sRNAs GlmZ and GlmY. *Nucleic Acids Res. 40*, 8021−8032.

(18) Soper, T. J., and Woodson, S. A. (2008) The rpoS mRNA leader recruits Hfq to facilitate annealing with DsrA sRNA. *RNA 14*, 1907−1917.

(19) Salim, N. N., and Feig, A. L. (2010) An upstream Hfq binding site in the fhlA mRNA leader region facilitates the OxyS-fhlA interaction. *PLoS One 5* (pii), e13028.

(20) Peng, Y., Curtis, J. E., Fang, X., and Woodson, S. A. (2014) Structural model of an mRNA in complex with the bacterial chaperone Hfq. *Proc. Natl. Acad. Sci. U. S. A. 111*, 17134−17139.

(21) Panja, S., Schu, D. J., and Woodson, S. A. (2013) Conserved arginines on the rim of Hfq catalyze base pair formation and exchange. *Nucleic Acids Res. 41*, 7536−7546.

(22) Zhang, A., Schu, D. J., Tjaden, B. C., Storz, G., and Gottesman, S. (2013) Mutations in interaction surfaces differentially impact E. coli Hfq association with small RNAs and their mRNA targets. *J. Mol. Biol. 425*, 3678−3697.

(23) Hussein, R., and Lim, H. N. (2011) Disruption of small RNA signaling caused by competition for Hfq. *Proc. Natl. Acad. Sci. U. S. A. 108*, 1110−1115.

(24) Moon, K., and Gottesman, S. (2011) Competition among Hfq-binding small RNAs in Escherichia coli. *Mol. Microbiol. 82*, 1545−1562.

(25) Fender, A., Elf, J., Hampel, K., Zimmermann, B., and Wagner, E. G. (2010) RNAs actively cycle on the Sm-like protein Hfq. *Genes Dev. 24*, 2621−2626.

(26) Olejniczak, M. (2011) Despite similar binding to the Hfq protein regulatory RNAs widely differ in their competition performance. *Biochemistry 50*, 4427−4440.

(27) Wagner, E. G. (2013) Cycling of RNAs on Hfq. *RNA Biol. 10*, 619−626.

(28) Ishikawa, H., Otaka, H., Maki, K., Morita, T., and Aiba, H. (2012) The functional Hfq-binding module of bacterial sRNAs consists of a double or single hairpin preceded by a U-rich sequence and followed by a 3′ poly(U) tail. *RNA 18*, 1062−1074.

(29) Brescia, C. C., Mikulecky, P. J., Feig, A. L., and Sledjeski, D. D. (2003) Identification of the Hfq-binding site on DsrA RNA: Hfq binds without altering DsrA secondary structure. *RNA 9*, 33−43.

(30) Møller, T., Franch, T., Hojrup, P., Keene, D. R., Bachinger, H. P., Brennan, R. G., and Valentin-Hansen, P. (2002) Hfq: a bacterial Sm-like protein that mediates RNA-RNA interaction. *Mol. Cell 9*, 23−30.

(31) Henderson, C. A., Vincent, H. A., Casamento, A., Stone, C. M., Phillips, J. O., Cary, P. D., Sobott, F., Gowers, D. M., Taylor, J. E., and Callaghan, A. J. (2013) Hfq binding changes the structure of Escherichia coli small noncoding RNAs OxyS and RprA, which are involved in the riboregulation of rpoS. *RNA 19*, 1089−1104.

(32) Milligan, J. F., Groebe, D. R., Witherell, G. W., and Uhlenbeck, O. C. (1987) Oligoribonucleotide synthesis using T7 RNA polymerase and synthetic DNA templates. *Nucleic Acids Res. 15*, 8783−8798.

(33) Hirel, P. H., Schmitter, M. J., Dessen, P., Fayat, G., and Blanquet, S. (1989) Extent of N-terminal methionine excision from *Escherichia coli* proteins is governed by the side-chain length of the penultimate amino acid. *Proc. Natl. Acad. Sci. U. S. A. 86*, 8247−8251.

(34) Wong, I., and Lohman, T. M. (1993) A double-filter method for nitrocellulose-filter binding: application to protein-nucleic acid interactions. *Proc. Natl. Acad. Sci. U. S. A. 90*, 5428−5432.

(35) Fahlman, R. P., and Uhlenbeck, O. C. (2004) Contribution of the esterified amino acid to the binding of aminoacylated tRNAs to the ribosomal P- and A-sites. *Biochemistry 43*, 7575−7583.

(36) Faner, M. A., and Feig, A. L. (2013) Identifying and characterizing Hfq-RNA interactions. *Methods 63*, 144−159.

(37) Updegrove, T. B., Correia, J. J., Chen, Y., Terry, C., and Wartell, R. M. (2011) The stoichiometry of the *Escherichia coli* Hfq protein bound to RNA. *RNA 17*, 489−500.

(38) Darfeuille, F., Unoson, C., Vogel, J., and Wagner, E. G. (2007) An antisense RNA inhibits translation by competing with standby ribosomes. *Mol. Cell 26*, 381−392.

(39) Andrade, J. M., Pobre, V., and Arraiano, C. M. (2013) Small RNA modules confer different stabilities and interact differently with multiple targets. *PLoS One 8*, e52866.

(40) Rasmussen, A. A., Johansen, J., Nielsen, J. S., Overgaard, M., Kallipolitis, B., and Valentin-Hansen, P. (2009) A conserved small RNA promotes silencing of the outer membrane protein YbfM. *Mol. Microbiol. 72*, 566−577.

(41) Fratczak, A., Kierzek, R., and Kierzek, E. (2011) Isoenergetic microarrays to study the structure and interactions of DsrA and OxyS RNAs in two- and three-component complexes. *Biochemistry 50*, 7647−7665.

(42) Altuvia, S., Weinstein-Fischer, D., Zhang, A., Postow, L., and Storz, G. (1997) A small, stable RNA induced by oxidative stress: role as a pleiotropic regulator and antimutator. *Cell 90*, 43−53.

(43) Balbontin, R., Fiorini, F., Figueroa-Bossi, N., Casadesus, J., and Bossi, L. (2010) Recognition of heptameric seed sequence underlies multi-target regulation by RybB small RNA in Salmonella enterica. *Mol. Microbiol. 78*, 380−394.

(44) Reuter, J. S., and Mathews, D. H. (2010) RNAstructure: software for RNA secondary structure prediction and analysis. *BMC bioinformatics 11*, 129.

(45) Thomason, M. K., Fontaine, F., De Lay, N., and Storz, G. (2012) A small RNA that regulates motility and biofilm formation in

response to changes in nutrient availability in Escherichia coli. *Mol. Microbiol.* 84, 17−35.

(46) Lease, R. A., and Woodson, S. A. (2004) Cycling of the Sm-like protein Hfq on the DsrA small regulatory RNA. *J. Mol. Biol.* 344, 1211−1223.

(47) Sledjeski, D. D., Whitman, C., and Zhang, A. (2001) Hfq is necessary for regulation by the untranslated RNA DsrA. *J. Bacteriol.* 183, 1997−2005.

(48) de Haseth, P. L., and Uhlenbeck, O. C. (1980) Interaction of Escherichia coli host factor protein with Q beta ribonucleic acid. *Biochemistry* 19, 6146−6151.

(49) Ross, J. A., Ellis, M. J., Hossain, S., and Haniford, D. B. (2013) Hfq restructures RNA-IN and RNA-OUT and facilitates antisense pairing in the Tn10/IS10 system. *RNA* 19, 670−684.

(50) Wang, W., Wang, L., Zou, Y., Zhang, J., Gong, Q., Wu, J., and Shi, Y. (2011) Cooperation of *Escherichia coli* Hfq hexamers in DsrA binding. *Genes Dev.* 25, 2106−2117.

(51) Arluison, V., Mura, C., Guzman, M. R., Liquier, J., Pellegrini, O., Gingery, M., Regnier, P., and Marco, S. (2006) Three-dimensional structures of fibrillar Sm proteins: Hfq and other Sm-like proteins. *J. Mol. Biol.* 356, 86−96.

(52) Olejniczak, M., Dale, T., Fahlman, R. P., and Uhlenbeck, O. C. (2005) Idiosyncratic tuning of tRNAs to achieve uniform ribosome binding. *Nat. Struct Mol. Biol.* 12, 788−793.

(53) Schrader, J. M., Chapman, S. J., and Uhlenbeck, O. C. (2009) Understanding the sequence specificity of tRNA binding to elongation factor Tu using tRNA mutagenesis. *J. Mol. Biol.* 386, 1255−1264.

(54) Rolle, K., Zywicki, M., Wyszko, E., Barciszewska, M. Z., and Barciszewski, J. (2006) Evaluation of the dynamic structure of DsrA RNA from E. coli and its functional consequences. *J. Biochem* 139, 431−438.

(55) Soper, T. J., Doxzen, K., and Woodson, S. A. (2011) Major role for mRNA binding and restructuring in sRNA recruitment by Hfq. *RNA* 17, 1544−1550.

(56) Papenfort, K., Said, N., Welsink, T., Lucchini, S., Hinton, J. C., and Vogel, J. (2009) Specific and pleiotropic patterns of mRNA regulation by ArcZ, a conserved, Hfq-dependent small RNA. *Mol. Microbiol.* 74, 139−158.

(57) Chao, Y., Papenfort, K., Reinhardt, R., Sharma, C. M., and Vogel, J. (2012) An atlas of Hfq-bound transcripts reveals 3′ UTRs as a genomic reservoir of regulatory small RNAs. *EMBO J.* 31, 4005−4019.

(58) Updegrove, T., Wilf, N., Sun, X., and Wartell, R. M. (2008) Effect of Hfq on RprA-rpoS mRNA pairing: Hfq-RNA binding and the influence of the 5′ rpoS mRNA leader region. *Biochemistry* 47, 11184−11195.

(59) Kovach, A. R., Hoff, K. E., Canty, J. T., Orans, J., and Brennan, R. G. (2014) Recognition of U-rich RNA by Hfq from the Gram-positive pathogen Listeria monocytogenes. *RNA* 20, 1548−1559.

(60) Robinson, K. E., Orans, J., Kovach, A. R., Link, T. M., and Brennan, R. G. (2014) Mapping Hfq-RNA interaction surfaces using tryptophan fluorescence quenching. *Nucleic Acids Res.* 42, 2736−2749.